*Supporting Information for*

# Molecular Insight into Intrinsic-Trap-Mediated Emission from Atomically Precise Copper-based Chalcogenide Models

Yi-Lei Xu,†[a] Yayun Ding,†[b] Lin-Mei Zhang,[a] Hao Ma,[a] Jia-Xing Liu,[a] Jiaxu Zhang,[b] Rui Zhou,[a,c] Dong-Sheng Li,[d] Shang-Fu Yuan,*[a] and Tao Wu*[a,b]

[a] *College of Chemistry and Materials Science, Guangdong Provincial Key Laboratory of Functional Supramolecular Coordination Materials and Applications, Jinan University, Guangzhou 510632, China.*

[b] *College of Chemistry, Chemical Engineering and Materials Science, Soochow University, Suzhou, Jiangsu 215123, China.*

[c] *Department of Developmental and Regenerative Biology, Jinan University, Guangzhou 510632, China.*

[d] *College of Materials and Chemical Engineering, Hubei Provincial Collaborative Innovation Centre for New Energy Microgrid, Key Laboratory of Inorganic Nonmetallic Crystalline and Energy Conversion Materials, China Three Gorges University, Yichang 443002, China.*

E-mail: *sfyuan@jnu.edu.cn*; *wutao@jnu.edu.cn*

# I. Experimental Section

**Chemicals and Materials.** All chemicals employed were analytical grade and commercially available. The reagents were used without further purification.

**Synthesis of 1-CuInS.** A mixture of copper iodide (32 mg, 0.17 mmol), indium powder (114 mg, 1.00 mmol), sulfur powder (120 mg, 3.75 mmol), antimony sulfide (42 mg, 0.12 mmol), deionized water ($H_2O$, 1.0 mL), 2-(2-aminoethylamino)ethanol (AEAE, 1.0 mL), 1,8-diazabicyclo[5.4.0] undec-7-ene (DBU, 2.0 mL) were stirred in a 23 mL Teflon-lined stainless-steel autoclave for twenty minutes. After the vessel was sealed and heated at 180 °C for 8 days, the autoclave was taken out and gradually cooled to room temperature. The orange block crystals were obtained by filtration, washed with ethanol for three times, and dried in vacuum. The phase purity of the sample was identified by powder X-ray diffraction measurements. The molecular formula of **1-CuInS** was determined to be $[(DBU\text{-}H)_{10.5}(AEAE\text{-}H)_{3.5}]$ $\{[Cu_5In_{30}S_{56}][InSb_4S_6]\}\cdot(H_2O)_{10}$.

**Synthesis of 1-CuGaS.** A mixture of copper iodide (32 mg, 0.17 mmol), gallium oxide (94 mg, 0.50 mmol), sulfur powder (120 mg, 3.75 mmol), antimony sulfide (36 mg, 0.11 mmol), deionized water ($H_2O$, 1.0 mL), tetraethylenepentamine (TEPA, 1.0 mL), tripropylamine (TPA, 1.0 mL), and piperidine (PR, 1.0 mL) were stirred in a 23 mL Teflon-lined stainless-steel autoclave for twenty minutes. After the vessel was sealed and heated at 180 °C for 8 days, the autoclave was taken out and gradually cooled to room temperature. A large number of yellow block crystals were obtained after three times of ethanol ultrasonic washing, filtration and dried in vacuum. The phase purity of the sample was identified by powder X-ray diffraction measurements. The molecular formula of **1-CuGaS** was determined to be $[(TEPA\text{-}2H)_5(TPA\text{-}H)_2(PR\text{-}H)_2]$ $\{[Cu_5Ga_{30}S_{56}][GaSb_4S_6]\}\cdot(H_2O)_8$.

**Synthesis of 2-CuGaS.** A mixture of copper acetate monohydrate (32 mg, 0.17 mmol), gallium oxide (94 mg, 0.50 mmol), sulfur powder (120 mg, 3.75 mmol), antimony acetate (48 mg, 0.16 mmol), deionized water ($H_2O$, 1.0 mL), tetraethylenepentamine

(TEPA, 1.0 mL) and triethylamine (TEA, 1.0 mL), 1,1,3,3-tetramethylguanidine (TMG, 1.0 mL) were stirred in a 23 ml Teflon-lined stainless-steel autoclave for twenty minutes. After the vessel was sealed and heated at 180 °C for 8 days, the autoclave was taken out and gradually cooled to room temperature. Yellow hexagonal crystals were obtained after three times of ethanol ultrasonic washing, filtration and dried in vacuum. The phase purity of the sample was identified by powder X-ray diffraction measurements. The molecular formula of **2-CuGaS** was determined to be $[(TEPA\text{-}2H)_6(TEA\text{-}H)_{1.5}(TMG\text{-}H)_{0.5}]\{[Cu_5Ga_{30}S_{56}]Sb\}\cdot(H_2O)_8$.

**Synthesis of 1-CuInGaS.** A mixture of copper iodide (32 mg, 0.17 mmol), indium powder (74 mg, 0.65 mmol), gallium oxide (40 mg, 0.21 mmol), sulfur powder (120 mg, 3.75 mmol), antimony acetate (48 mg, 0.16 mmol), deionized water ($H_2O$, 1.0 mL), 2-(2-aminoethylamino)ethanol (AEAE, 1.0 mL), 1,8-diazabicyclo[5.4.0] undec-7-ene (DBU, 2.0 mL) were stirred in a 23 ml Teflon-lined stainless-steel autoclave for twenty minutes. After the vessel was sealed and heated at 180 °C for 8 days, the autoclave was taken out and gradually cooled to room temperature. A large number of yellow block crystals were obtained after three times of ethanol ultrasonic washing, filtration and dried in vacuum. The phase purity of the sample was identified by powder X-ray diffraction measurements.

**Synthesis of 1-CuInCdS@*n*.** A mixture of copper iodide (7 mg for $n$ = 1, 14 mg for $n$ = 2, 21 mg for $n$ = 3, 28 mg for $n$ = 4 ), cadmium nitrate tetrahydrate (42 mg for $n$ = 1, 32 mg for $n$ = 2, 22 mg for $n$ = 3, 12 mg for $n$ = 4), indium powder (114 mg, 1.00 mmol), sulfur powder (120 mg, 3.75 mmol), antimony sulfide (28 mg, 0.08 mmol), deionized water ($H_2O$, 1.0 mL), 2-(2-aminoethylamino)ethanol (AEAE, 1.0 mL), 1,8-diazabicyclo[5.4.0]undec-7-ene (DBU, 2.0 mL) was stirred in a 23 mL Teflon-lined stainless-steel autoclave for twenty minutes. After the vessel was sealed and heated at 180 °C for 8 days, the autoclave was taken out and gradually cooled to room temperature. Octahedral crystals were obtained after three times of ethanol ultrasonic washing, filtration and dried in vacuum. The phase purity of the sample was identified by powder X-ray diffraction measurements.

## II. Physical measurements

**X-ray Crystallography.** The single-crystal X-ray diffraction (SCXRD) measurements on **1-CuInS**, **1-CuGaS**, and **2-CuGaS** were performed on a Bruker Smart CPAD area diffractometer with nitrogen-flow temperature controller using graphite-monochromated MoKα (λ = 0.71073 Å) radiation at 120 K. The structures were solved by direct method using SHELXS-2014 and refined anisotropically by least-squares on $F^2$ using the SHELXTL program. SQUEEZE routine in PLATON was employed in the structural refinements. There is a level A alert "The value of sine (theta_max)/wavelength is less than 0.550" for **1-CuInS** and **1-CuGaS**. A full set of the crystallography data of this compound was collected. However, the high angle data was dominated by noise [I/sigma < 2.0] and was omit by collecting relatively low resolution for high-quality crystal data.

**Powder X-ray Diffraction Characterization.** The powder X-ray diffraction (PXRD) data of **1-CuInS**, **1-CuGaS**, and **2-CuGaS** were collected on a diffractometer (D2 PHASER, Bruker, Germany) utilizing Cu-Kα (λ = 1.54184 Å) radiation operated at 30 kV and 10 mA. The samples were ground into fine powders for several minutes before the test.

**Elemental Analysis.** Energy dispersive spectroscopy (EDS) was measured on scanning electron microscope (SEM) equipped with energy dispersive spectroscopy (EDS) detector operated at an accelerating voltage of 25 kV and 30 s accumulation time. Elemental analysis of C, H, and N was measured on VARIO EL III elemental analyzer (**1-CuInS**, *Calcd.* (*wt*%): C, 15.31; N, 4.60; H, 2.89; *Found* (*wt*%): C, 14.92; N, 4.51; H, 2.57. **1-CuGaS**, *Calcd.* (*wt*%): C, 12.53; N, 6.23; H, 3.23; *Found* (*wt*%): C, 12.03; N, 6.31; H, 2.90. **2-CuGaS**, *Calcd.* (*wt*%): C, 12.26; N, 7.93; H, 3.40; *Found* (*wt*%): C, 12.69; N, 7.72; H, 3.18.)

**Thermogravimetric analysis (TGA).** The thermogravimetric (TG) curves of **1-CuInS**, **1-CuGaS**, and **2-CuGaS** were measured on a Shimadzu TGA-50 thermal

analyzer by heating samples from room temperature to 800 ℃ at 10 ℃/min under $N_2$ flow.

**Diffuse Reflectance Spectra.** The solid-state UV-Vis diffusion reflectance spectra of **1-CuInS**, **1-CuGaS**, and **2-CuGaS** were measured on a SHIMADZU UV-3600 UV-Vis-NIR spectrophotometer equipped with an integrating sphere by using $BaSO_4$ powder as the reflectance reference. In order to determine the band edge of the direct-gap semiconductor, the relation between the absorption coefficients ($\alpha$) and the incident photon energy ($h\nu$) is exhibited as $\alpha h\nu = A(h\nu - Eg)^{0.5}$, where A is a constant that relates to the effective masses associated with the valence and conduction bands, and $Eg$ is the optical transition gap of the solid material. By extrapolating the linear region to the abscissa, the band gap $Eg$ can be estimated.

**X-ray Photoelectron Spectroscopy**. X-ray photoelectron spectroscopy (XPS) was collected with a Leeman prodigy spectrometer equipped with a monochromatic Al K$\alpha$ X-ray source and a concentric hemispherical analyzer. All binding energies were calibrated using the C (1s) carbon peak (284.8 eV), which was applied as an internal standard.

**Ultraviolet Photoelectron Spectroscopy.** Ultraviolet photoemission spectroscopy (UPS) was measured on a Escalab 250Xi spectrometer. For UPS measurements, He I (21.22 eV) radiation line from a discharge lamp was used, and all the UPS measurements of the onset of photoemission were done using standard procedures with a -10 V bias applied to the sample.

**Photoluminescence and Photoluminescence Excitation Spectra.** Photoluminescence (PL) and photoluminescent excitation (PLE) spectra were measured by a HORIBA scientific Fluorolog-3 steady state and time-resolved fluorescence spectrophotometer coupled with a 450 W xenon lamp. PL decays were recorded using a HORIBA scientific Fluorolog-3 steady state fluorimeter with a time-correlated single-photon counting (TCSPC) spectrometer and a pulsed xenon lamp as the excitation source. Low temperature PL spectra were recorded on a HORIBA scientific Fluorolog-3

spectrophotometer with a low temperature accessory.

## III. Supporting figures

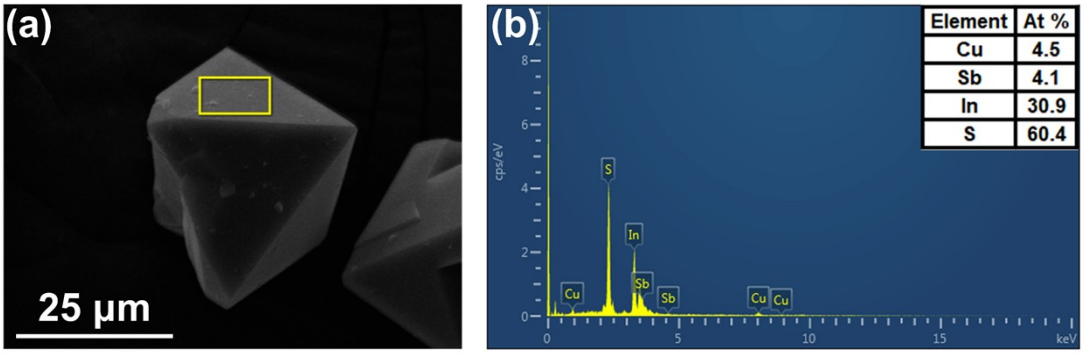


**Figure S1.** (a) SEM image and (b) EDS pattern of as-synthesized **1-CuInS** crystal (the ratio of Cu/Sb/In *Calcd*: 1.00/0.80/6.20; *Found*: 1.00/0.91/6.87).

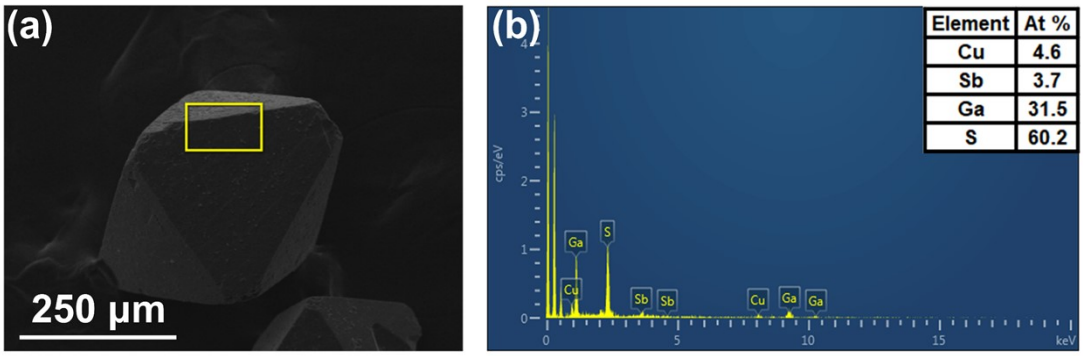


**Figure S2.** (a) SEM image and (b) EDS pattern of **1-CuGaS** (the ratio of Cu/Sb/Ga *Calcd*: 1.00/0.80/6.20; *Found*: 1.00/0.80/6.87).

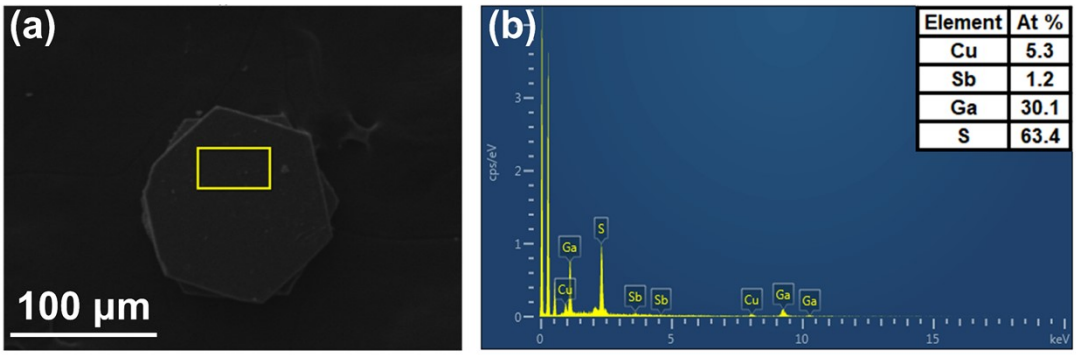


**Figure S3.** (a) SEM image and (b) EDS pattern of as-synthesized **2-CuGaS** crystal (the ratio of Cu/Sb/Ga *Calcd*: 1.00/0.20/6.00; *Found*: 1.00/0.23/5.68).

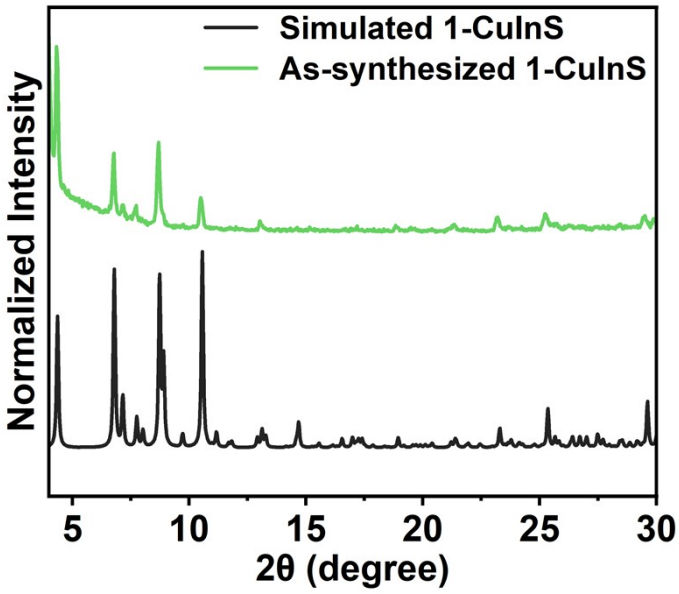


**Figure S4.** The simulated and experimental PXRD patterns of **1-CuInS**.

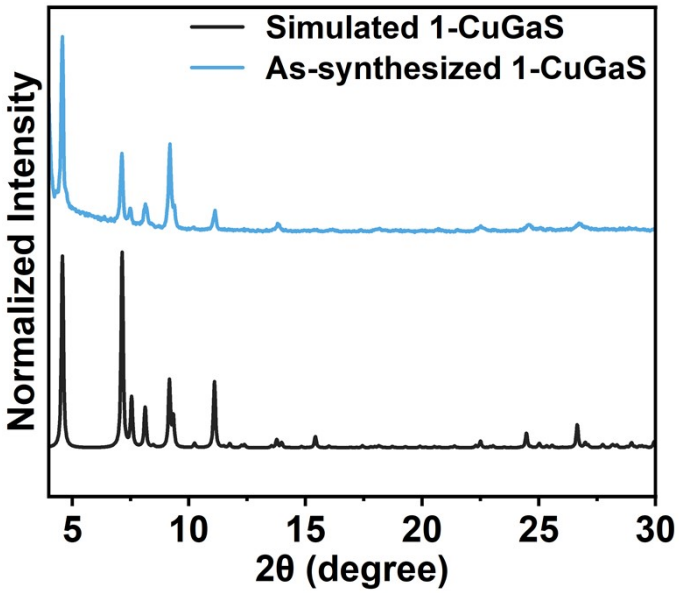


**Figure S5.** The simulated and experimental PXRD patterns of **1-CuGaS**.

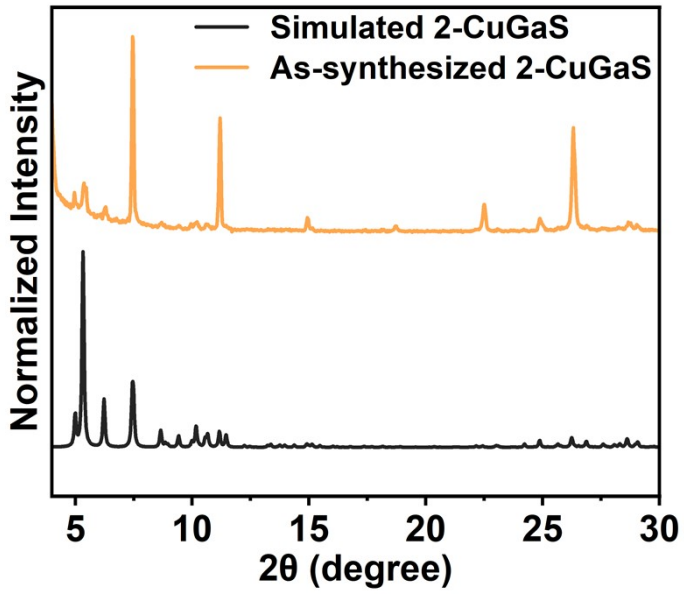


**Figure S6.** The simulated and experimental PXRD patterns of **2-CuGaS**.

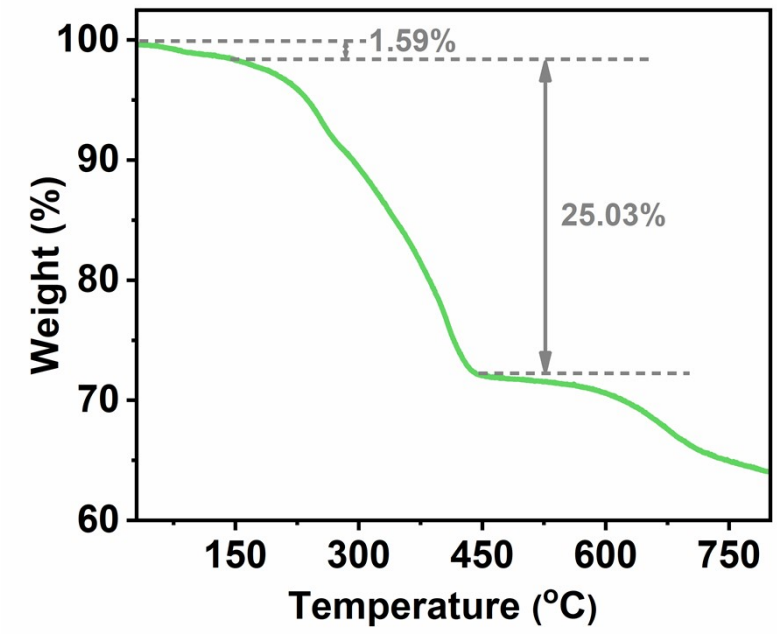


**Figure S7.** TGA curve of **1-CuInS**.

The first weight loss of 1.59% (sim. 2.12%) (below 140 °C) could be attributed to the desorption of water molecules. The abrupt weight loss of about 25.03% (sim. 23.11%) occurs between 140-420 °C, corresponding to the removal of charge-balanced organic amine molecules.

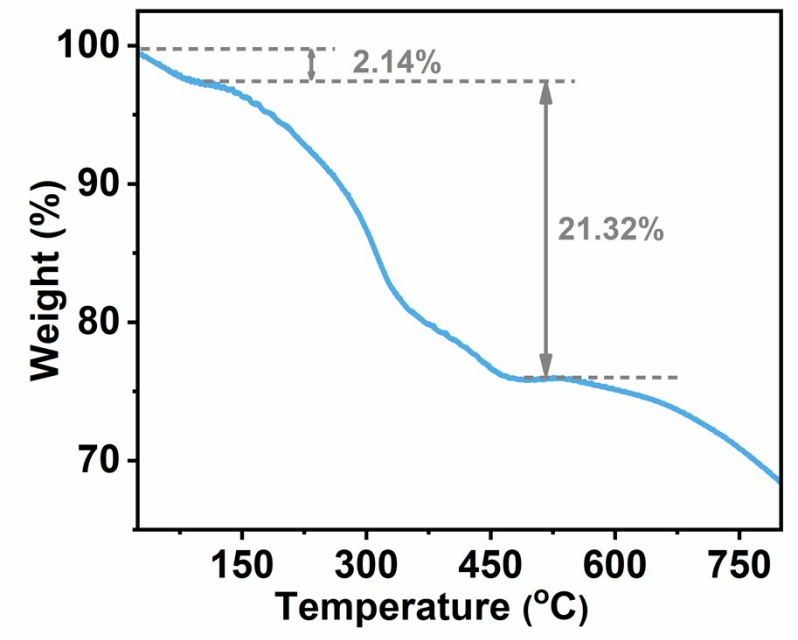


**Figure S8.** TGA curve of **1-CuGaS**.

The first weight loss of 2.14% (sim. 2.22%) could be attributed to the desorption of water molecules. The abrupt weight loss of around 21.32% (21.61%) occurs between 100-460 °C, corresponding to removal of charge-balanced organic amine molecules.

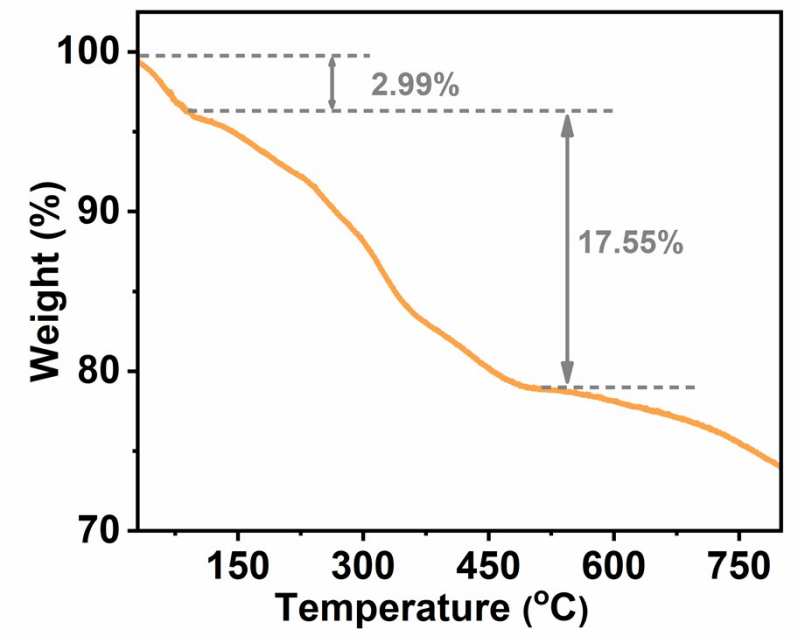


**Figure S9.** TGA curves of **2-CuGaS**.

The first weight loss of 2.99% (sim. 2.48%) could be attributed to the loss of water

molecules. The abrupt weight loss of around 17.55% (23.14%) occurs between 100-485 °C, corresponding to removal of charge-balanced organic amine molecules.

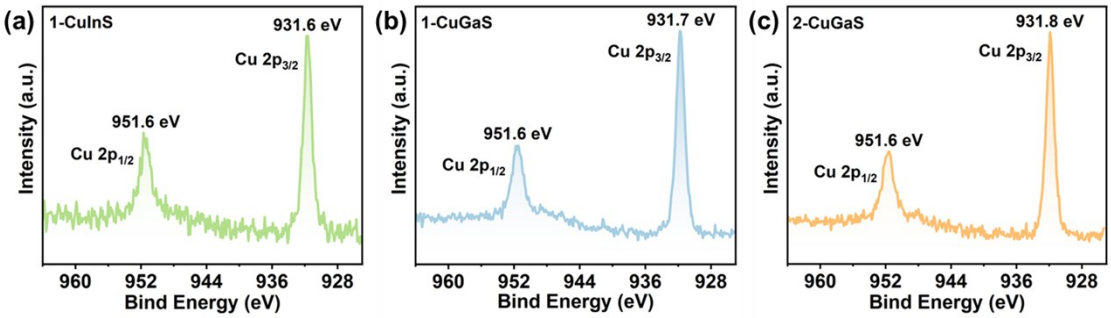


**Figure S10.** Cu 2p high resolution XPS spectra of **1-CuInS** (a), **1-CuGaS** (b) and **2-CuGaS** (c).

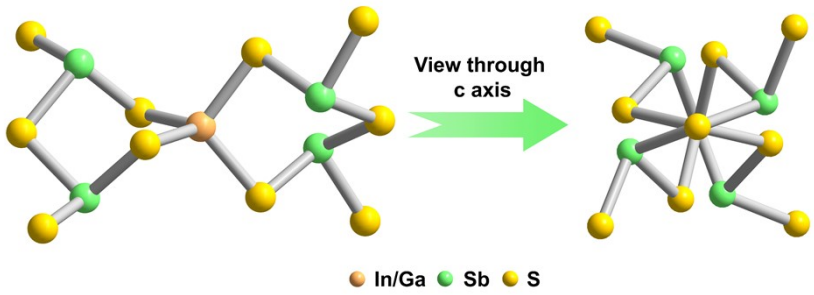


**Figure S11.** [$MSb_4S_{10}$] unit in **1-CuInS** and **1-CuGaS** (for **1-CuInS**, M = In; for **1-CuGaS**, M = Ga).

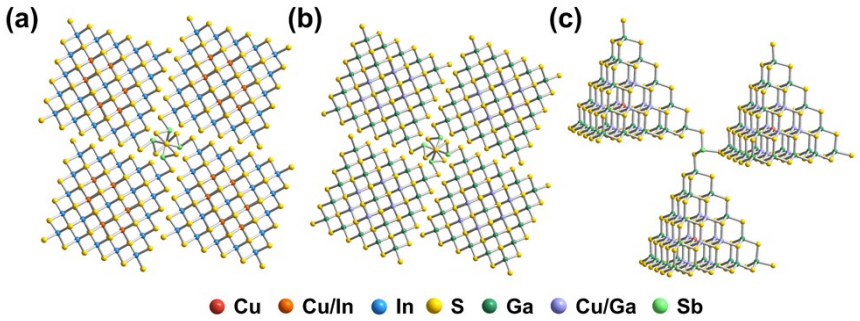


**Figure S12.** (a) The [$InSb_4S_{10}$] linker tetrahedrally bonded to four T5-CuInS NCs in **1-CuInS**, (b) The [$GaSb_4S_{10}$] linker tetrahedrally bonded to four T5-CuGaS NCs in **1-CuGaS**, (c) The [$SbS_3$] linker bonded to three T5-CuGaS NCs in **2-CuGaS**.

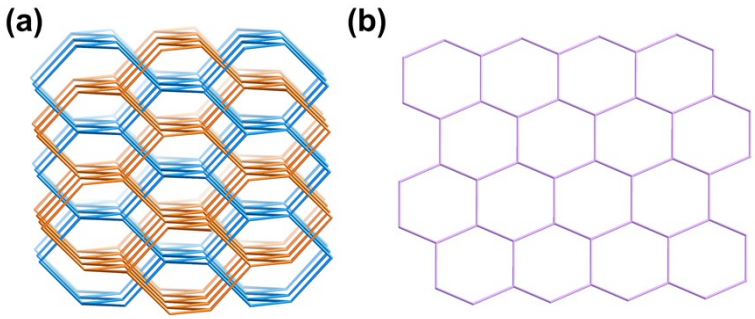


**Figure S13.** (a) The simplified double-interpenetrated *dia* topology of **1-CuInS** and **1-CuGaS**. (b) The simplified *hcb* topology of **2-CuGaS**.

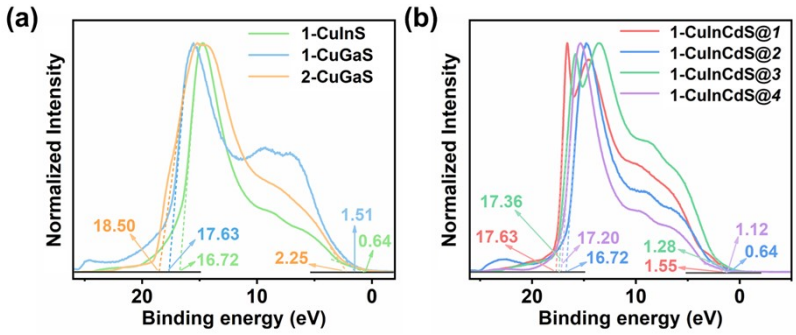


**Figure S14.** (a) UPS spectrum of **1-CuInS**, **1-CuGaS**, and **2-CuGaS**; (b) **1-CuInCdS@*n*** (n = 1-4). The values of the left part of the spectrum are the secondary electron cutoff of the samples and the values of the right part indicate the energy of the Highest Occupied State (HOS).

The valence band position was determined according to the previous method.[1] The ionization potential (equivalent to the valence band energy) of **1-CuInS** was calculated to be 5.14 eV by subtracting the width of the He I UPS spectra from the excitation energy (21.22 eV). Accordingly, the valence band energy is estimated to be 5.10 eV for **1-CuGaS**, and 4.97 eV for **2-CuGaS**; and 5.14 eV for all the four samples of **1-CuInCdS@*n*** (n = 1-4).

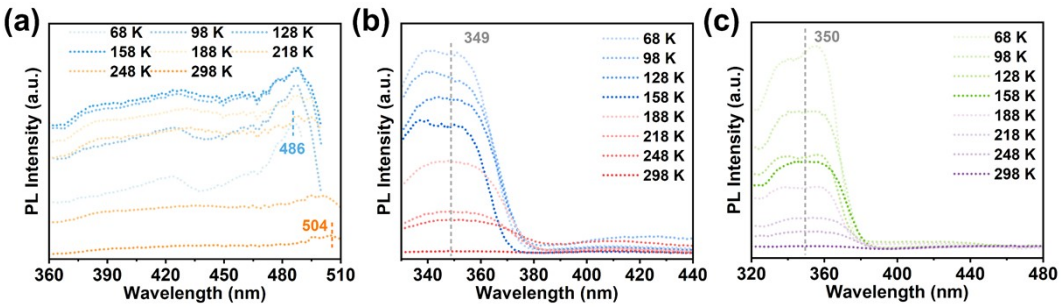


**Figure S15.** Temperature-dependent PLE spectra of **1-CuInS** (a), **1-CuGaS** (b), and **2-CuGaS** (c).

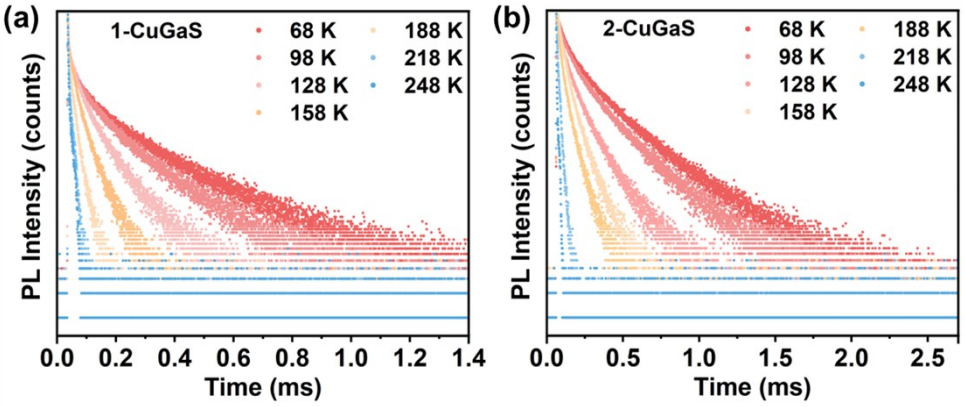


**Figure S16.** Temperature-dependent PL decay curves of **1-CuGaS** (a) and **2-CuGaS** (b).

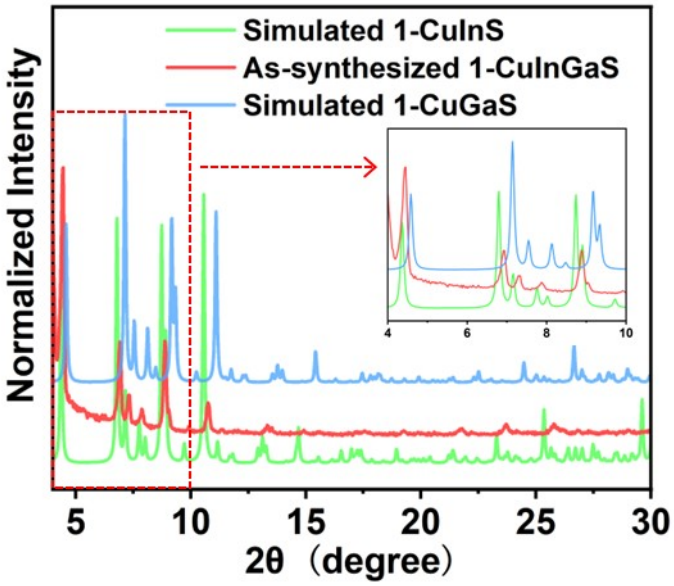


**Figure S17.** Comparison of the experimental PXRD patterns of **1-CuInGaS** and the simulated PXRD patterns of **1-CuInS** and **1-CuGaS**. The inset is an enlarged one for clarity.

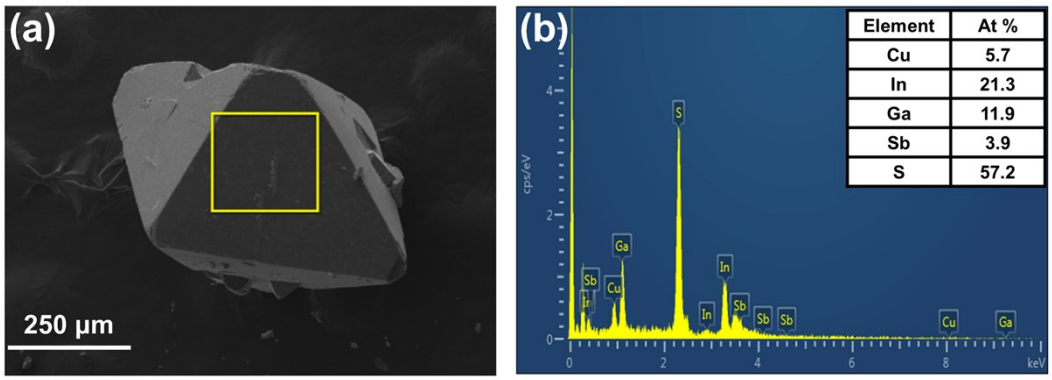


**Figure S18.** (a) SEM image and (b) EDS pattern of as-synthesized **1-CuInGaS** crystal.

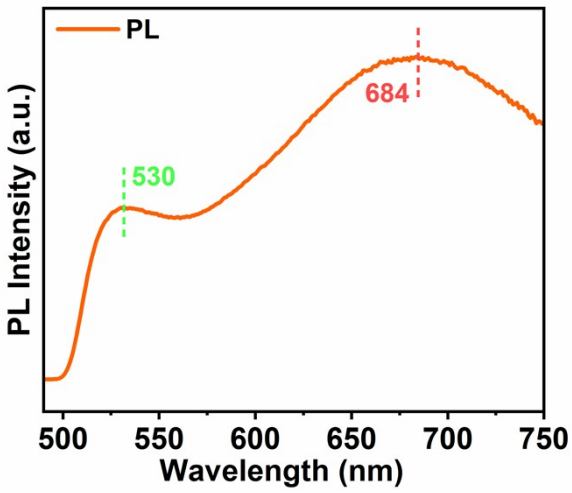


**Figure S19.** Room-temperature (RT) PL spectra of **1-CuInGaS** under the excitation of 450 nm.

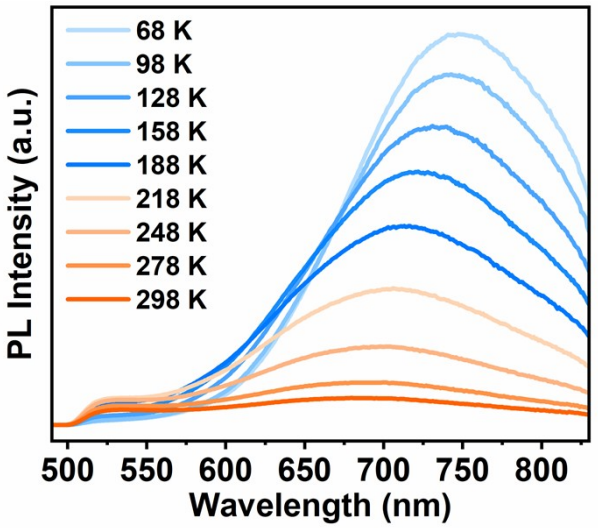


**Figure S20.** Temperature-dependent PL spectra of **1-CuInGaS** under the excitation of 450 nm.

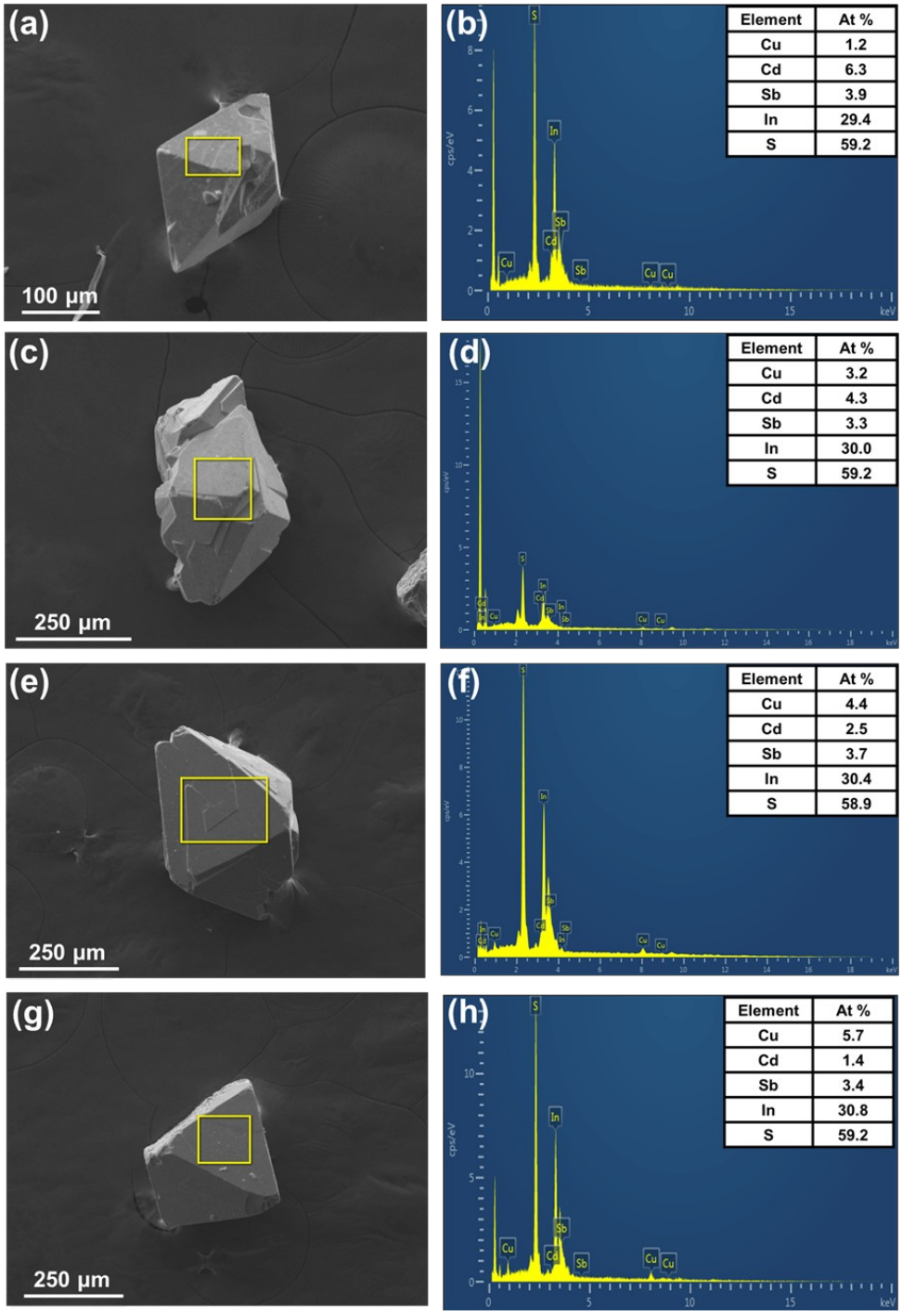


**Figure S21.** SEM image of as-synthesized **1-CuInCdS@*1*** (a), **1-CuInCdS@*2*** (c), **1-CuInCd@*3*** (e), and **1-CdCuIn@*4*** (g). EDS patterns of **1-CuInCdS@*1*** (b), **1-CuInCdS@*2*** (d), **1-CuInCd@*3*** (f), and **1-CdCuIn@*4*** (h).

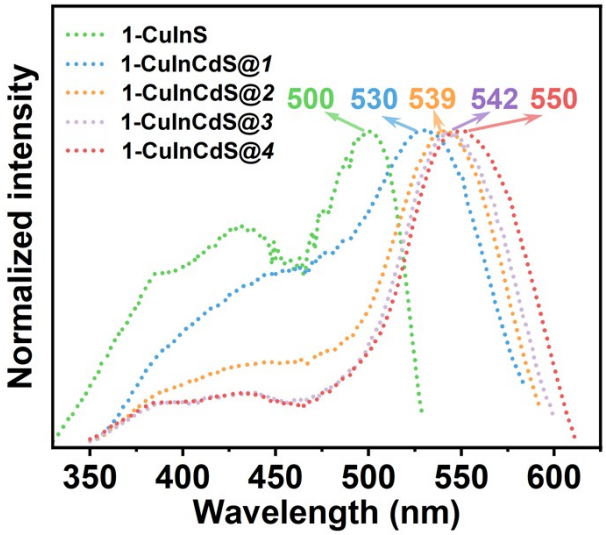


**Figure S22.** RT PLE spectra of as-synthesized **1-CuInS** and **1-CuInCdS@*n*** (*n* = 1-4).

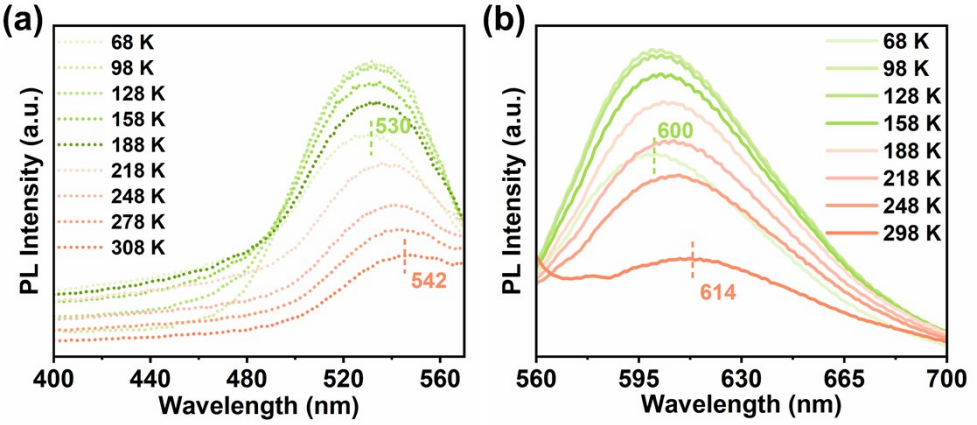


**Figure S23.** (a) Temperature-dependent PLE spectra of **1-CuInCdS@*2*.** (b) Temperature-dependent PL spectra of **1-CuInCdS@*2*.**

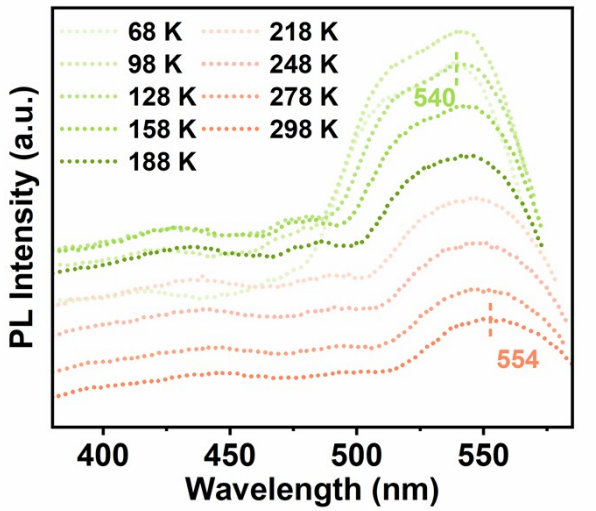


**Figure S24.** Temperature-dependent PLE spectra of **1-CuInCdS@*4***.

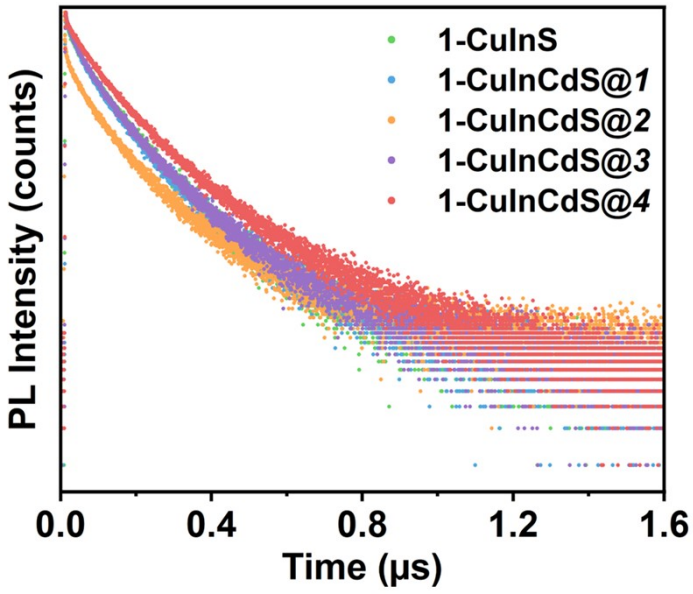


**Figure S25.** RT PL decay curves of **1-CuInS** and **1-CuInCdS@*n*** (*n* = 1-4).

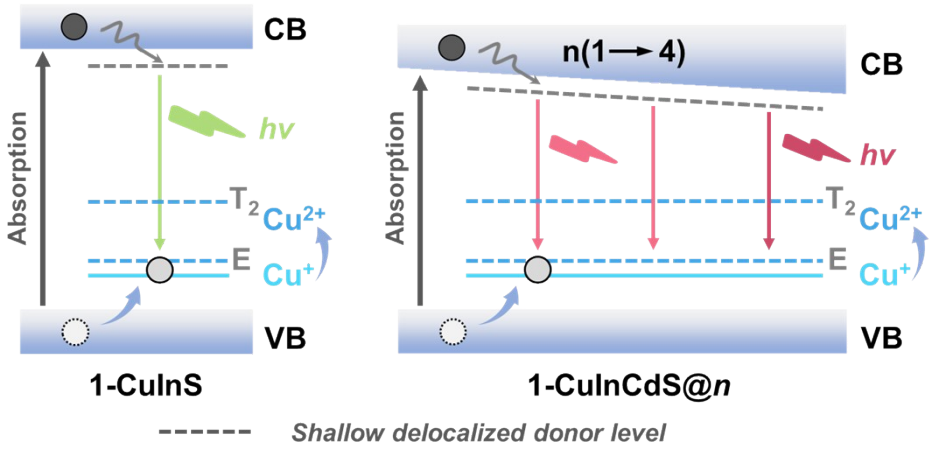


**Figure S26.** Proposed energy level diagram for **1-CuInS** and **1-CuInCdS@*n***. (VB: valence band, CB: conduction band). The introduction of Cd into the framework of **1-CuInS** resulted in the redshift of the shallow delocalized trap sites as well as the CB state.

**Table S1**. Crystallographic data and structure refinement parameters for **1-CuInS**, **1-CuGaS**, and **2-CuGaS**.

| **Compounds** | **1-CuInS** | **1-CuGaS** | **2-CuGaS** |
|---|---|---|---|
| Framework Formula | $Cu_5In_{31}S_{62}Sb_4$ | $Cu_5Ga_{31}S_{62}Sb_4$ | $Cu_5Ga_{30}S_{56}Sb$ |
| Crystal system | tetragonal | tetragonal | hexagonal |
| Space group | $I4_1/a$ | $I4_1/a$ | $P6_3/m$ |
| $Z$ | 4 | 4 | 4 |
| $a$ (Å) | 22.760(3) | 21.7439(14) | 20.424(4) |
| $b$ (Å) | 22.760(3) | 21.7439(14) | 20.424(4) |
| $c$ (Å) | 44.026(6) | 41.698(3) | 47.512(10) |
| $\alpha$ (deg.) | 90 | 90 | 90.00(3) |
| $\beta$ (deg.) | 90 | 90 | 90.00(3) |
| $\gamma$ (deg.) | 90 | 90 | 120.00(3) |
| $V$ (Å$^3$) | 22807(6) | 19715(3) | 17164(8) |
| GOF on $F^2$ | 1.139 | 1.040 | 1.042 |
| $R_1$, $wR_2$ ($I > 2\sigma(I)$) | 0.0678, 0.2111 | 0.0546, 0.1720 | 0.0552, 0.1620 |
| $R_1$, $wR_2$ (all data) | 0.1079, 0.2870 | 0.0888, 0.2101 | 0.0712, 0.1777 |

**Table S2.** PL decay lifetime of **1-CuInS** and **1-CuInCdS@*n* (*n* = 1-4)** at 298 K.

| Sample | $A_1$ (%) | $\tau_1$ (ns) | $A_2$ (%) | $\tau_2$ (ns) | $A_3$ (%) | $\tau_3$ (ns) | $\tau_{ave}$ (ns) |
|---|---|---|---|---|---|---|---|
| **1-CuInS** | 63.25 | 94.9 | 5.64 | 16.1 | 31.11 | 217 | 128 |
| **1-CuInCdS@*1*** | 61.93 | 92.3 | 7.44 | 18.2 | 30.63 | 240 | 132 |
| **1-CuInCdS@*2*** | 38.39 | 60.1 | 3.57 | 1.05 | 58.04 | 185 | 130 |
| **1-CuInCdS@*3*** | 9.86 | 24.3 | 63.98 | 98.6 | 26.35 | 257 | 133 |
| **1-CuInCdS@*4*** | 57.99 | 90.6 | 9.14 | 19.3 | 32.87 | 265 | 141 |

**Table S3.** PL decay lifetime of **1-CuInS, 1-CuInCdS@*2***, and **1-CuInCdS@*4*** at 68 K.

| Sample | $A_1$ (%) | $\tau_1$ ( μ s) | $A_2$ (%) | $\tau_2$ (μs) | $\tau_{ave}$ (μs) |
|---|---|---|---|---|---|
| **1-CuInS** | 38.16 | 1.74 | 61.84 | 10.6 | 7.22 |
| **1-CuInCdS@*2*** | 32.76 | 1.52 | 67.24 | 10.7 | 7.70 |
| **1-CuInCdS@*4*** | 35.24 | 1.98 | 64.76 | 14.8 | 10.3 |

**Table S4.** PL decay lifetime of **1-CuGaS**.

| Temp. (K) | $A_1$ (%) | $\tau_1$ (μs) | $A_2$ (%) | $\tau_2$ (μs) | $A_3$ (%) | $\tau_3$ (μs) | $\tau_{ave}$ (μs) |
|---|---|---|---|---|---|---|---|
| **68** | 29.58 | 44.9 | 67.37 | 214 | 3.05 | 3.80 | 158 |
| **98** | 34.43 | 38.0 | 62.82 | 159 | 2.75 | 3.06 | 113 |
| **128** | 42.54 | 26.9 | 50.48 | 89.4 | 6.98 | 2.26 | 56.7 |
| **158** | 51.46 | 19.0 | 38.72 | 52.0 | 9.82 | 2.20 | 30.1 |
| **188** | 68.41 | 11.9 | 4.35 | 30.3 | 27.24 | 1.65 | 9.91 |
| **218** | 36.96 | 1.30 | 63.04 | 8.44 | - | - | 5.80 |
| **248** | 42.29 | 1.19 | 57.71 | 8.17 | - | - | 5.22 |

**Table S5.** PL decay lifetime of **2-CuGaS**.

| Temp. (K) | $A_1$ (%) | $\tau_1$ (μs) | $A_2$ (%) | $\tau_2$ (μs) | $A_3$ (%) | $\tau_3$ (μs) | $\tau_{ave}$ (μs) |
|---|---|---|---|---|---|---|---|
| **68** | 44.01 | 144 | 40.78 | 355 | 15.21 | 37.7 | 214 |
| **98** | 45.06 | 122 | 38.73 | 287 | 16.21 | 34.3 | 172 |
| **128** | 46.37 | 86.3 | 23.93 | 182 | 29.70 | 31.8 | 93.0 |
| **158** | 42.52 | 54.2 | 8.87 | 98.8 | 48.61 | 21.0 | 42.0 |
| **188** | 74.16 | 12.2 | 10.67 | 23.8 | 15.17 | 2.56 | 12.0 |
| **218** | 23.94 | 1.83 | 76.06 | 9.35 | - | - | 7.55 |
| **248** | 41.36 | 1.26 | 58.64 | 8.03 | - | - | 5.23 |

**Table S6.** PL decay lifetime of **1-CuInGaS** at 68 K.

| Emission position | $A_1$ (%) | $\tau_1$ (μs) | $A_2$ (%) | $\tau_2$ (μs) | $A_3$ (%) | $\tau_3$ (μs) | $\tau_{ave}$ (μs) |
|---|---|---|---|---|---|---|---|
| **747 nm** | 25.20 | 42.1 | 71.83 | 220 | 2.97 | 3.82 | 169 |
| **520 nm** | 54.37 | 10.6 | 31.70 | 21.9 | 13.93 | 1.78 | 13.0 |

**Table S7.** PL decay lifetime of **1-CuInGaS** at 298 K.

| Emission position | $A_1$ (%) | $\tau_1$ (ns) | $A_2$ (%) | $\tau_2$ (ns) | $A_3$ (%) | $\tau_3$ (ns) | $\tau_{ave}$ (ns) |
|---|---|---|---|---|---|---|---|
| **684nm** | 43.55 | 157 | 5.05 | 21.6 | 51.41 | 482 | 317 |
| **530 nm** | 73.99 | 88.3 | 12.71 | 235 | 13.30 | 18.9 | 97.7 |

**Table S8**. Molar ratio of Cu:Cd in **1-CuInCdS@*n*** (n = 1-4) samples determined by EDS measurements.

| Sample | Reactants | Average Molar Ratio of Cu:Cd |
|---|---|---|
| **1-CuInCdS@*1*** | 7 mg $Cu(OAc)_2 \cdot H_2O$<br>42 mg $Cd(NO_3)_2 \cdot 4H_2O$ | 1.2:6.3 |
| **1-CuInCdS@*2*** | 14 mg $Cu(OAc)_2 \cdot H_2O$<br>32 mg $Cd(NO_3)_2 \cdot 4H_2O$ | 3.2:4.3 |
| **1-CuInCdS@*3*** | 21 mg $Cu(OAc)_2 \cdot H_2O$<br>22 mg $Cd(NO_3)_2 \cdot 4H_2O$ | 4.4:2.5 |
| **1-CuInCdS@*4*** | 28 mg $Cu(OAc)_2 \cdot H_2O$<br>12 mg $Cd(NO_3)_2 \cdot 4H_2O$ | 5.7:1.4 |

**References:**

1. J. Liu, Y. Liu, N. Liu, Y. Han, X. Zhang, H. Huang, Y. Lifshitz, S.-T. Lee, J. Zhong and Z. Kang, Metal-free efficient photocatalyst for stable visible water splitting via a two-electron pathway. *Science*, 2015, **347,** 970-974.